IEEE Transactions on Nuclear Science, Vol. NS-32, No. 5, October 1985

# PENETRATION OF RF FIELDS INTO HOLES IN CAVITY WALLS

R.M. Hutcheon and R.A. Vokes
Atomic Energy of Canada Limited, Research Company
Chalk River Nuclear Laboratories
Chalk River, Ontario, Canada K0J 1J0

## Summary

Measurements of magnetic fields in cavity wall penetrations were made to provide engineering data for practical cavity design. The data were normalized to cavity wall fields and, as expected, when all coordinates were scaled by the transverse dimension of the penetration, the measured field distributions were similar and differed by only small systematic amounts. These data are thus generally applicable to any standard rf cavity, independent of frequency, provided only that the penetration, when regarded as a waveguide, is well below cutoff frequency. Until the results of three dimensional rf cavity codes are commonly available, these numbers should assist design engineers in detailing the properties of tuning plungers, drive loops, pumping ports and view ports.

## Introduction

The practical design of an rf cavity must include drive loops, field probes, vacuum pumping ports and observation windows. Specifying these requires knowledge of the penetration of rf fields into the various ports. At low rf power levels these fields are of little consequence, except possibly for their effect on the cavity Q, since the wall heating is negligible and the position of components in the penetrations can be easily modified. At high power levels, where cavity wall and component cooling is essential, an error in estimating the field penetration can, at the least, lead to costly design modifications and in the worst case to component overheating and destruction. To avoid such problems in the design of RFQ1, a high power cw proton accelerator[1,2] sets of measurements were made of the penetration of "outer wall" magnetic fields into circular and rectangular slots, excited well below cutoff.

The theory for waveguide transmission well below cutoff suggests that the magnitude and shape of these fields should scale with the transverse dimension of the penetration and be approximately independent of wavelength[3]. Thus the fields measured at one frequency and parameterized are also useful at other frequencies. The ultimate value of the curves is in their use for estimating fields, surface power levels, tuning plunger effects and the influence of ports on cavity Q.

## Measurement Technique

The measurements were performed using an upright cylindrical aluminum cavity (Fig. 1) (height = 1.00 m, radius, a, = 0.415 m) which was critically coupled via a magnetic drive loop to a transmission phase locked rf source. Using this technique, cavity frequency variations had no affect on the cavity power levels, which were carefully regulated. The $TM_{010}$ mode of excitation ($\lambda$ = 1.08 m, f = 270 MHz, $Q_0 \approx 42\,000$) was used exclusively in the experiment. The magnetic field lines form horizontal closed loops with maximum strength near the outer wall while the electric fields form vertical lines from one end plate to the other with zero strength on the outer wall. The radial dependence of the magnetic field is given explicitly by

$$B \propto J_1\left(\frac{2.405\ r}{a}\right) \qquad (1)$$

where $J_1$ is the first order Bessel function, and r is the radius in metres. The ratio of the field at the outer wall (r = 0.415 m) to the maximum field (r = 0.315 m) is 0.89.

A set of deep circular and rectangular waveguide-like penetrations, all with transverse dimensions less than 0.15 $\lambda$, were formed by adding appendages to the cylinder wall (Fig. 1). The penetrations thus were equivalent to waveguides driven well below cutoff by an almost pure transverse magnetic rf field. Two types of measurements were performed: some with appropriately shaped tuning plungers forming sliding shorts in the waveguide-like appendages, and others with "B" field probes (a loop on the end of a 9.5 mm diameter solid copper 50 ohm coaxial line) inserted horizontally into the appendages from the outside zero field region.

The tuning plunger "field" measurements are based on using the Slater perturbation theorem[4] to relate small changes in frequency caused by plunger displacement to small changes in magnetic stored energy using

$$\frac{\Delta f}{f_0} = \frac{1}{2}\ \frac{\int_{\Delta v} [\frac{1}{2}\mu_0 H_0{}^2 - \frac{1}{2}\varepsilon_0 E_0{}^2]dv}{[\text{Stored Energy}]} \qquad (2)$$

If the assumption is made that $E_0$ is negligible in and immediately around the appendages and that the stored energy remains constant (Q unchanged), then

$$[f(o) - f(Z)] \propto \int_{\Delta v} [B_0{}^2(r) - B^2(r)]dv \qquad (3)$$

where f(Z) is the frequency as a function of Z, the plunger face position, $\Delta v$ is the change in volume of the cavity and $B_0(r)^2$ is the field distribution squared, without the appendage (i.e., with the plunger face flush with the cavity wall, Z = 0). For a plunger displacement of $\Delta Z$ from position Z, equation (3) yields the appropriate relationship

$$\Delta f_Z = f(Z-\tfrac{\Delta Z}{2}) - f(Z+\tfrac{\Delta Z}{2}) \simeq [K * B_{eff}(Z)]^2 * \text{Area} * \Delta Z \qquad (4)$$

At Z = 0,

$$\Delta f_0 = f(-\tfrac{\Delta Z}{2}) - f(+\tfrac{\Delta Z}{2}) \simeq [K * B_{wall}]^2 * \text{Area} * \Delta Z \qquad (5)$$

where $B_{wall}$ is the unperturbed cavity wall field and yields the normalization of equation (4), giving

$$\frac{B_{eff}(Z)}{B_{wall}} = R = \left[\frac{\Delta f_Z}{\Delta f_0}\right]^{1/2} \qquad (6)$$

The magnetic field probe measurements were made with both transverse ($B_x$) and longitudinal ($B_Z$) field sensitive loops. The longitudinal loop was carefully constructed and oriented to be insensitive to $B_x$. Normalization of $B_x$ to the unperturbed tank wall field was done by inserting the probe ≈ 100 mm into the tank to the region of the unperturbed radial distribution maximum.

The $B_Z$ probe output was normalized to the transverse wall field by inserting it through a small hole in the $TM_{010}$ cavity wall and orienting the coax

0018-9499/85/1000-2772 $1.00 © 1985 Canadian Crown Copyright

line to be almost tangent to the tank wall so the plane of the loop was perpendicular to the magnetic wall field. The loop area correction factor is then only the cosine of a small angle (< 10°).

## Tuning Plunger Results and the "Wall Field Equivalent" Depth

In Fig. 1 are shown the ratios of effective hole field to unperturbed cavity wall field derived using equations (4) and (5) as a function of tuning plunger depth in three different port configurations. Note that, once the equivalent field has fallen below 75% of the wall field ($Z/W \approx 0.15$), the decrease is approximately exponential, with essentially the same exponent regardless of the port shape. The difference in zero displacement of the curves may be due to the imprecise definition of the $Z = 0$ point of the circular hole due to cavity wall curvature.

The tuning plunger measurements were also used to "calibrate" a method for estimating the frequency shift produced by a deep penetration in a cavity wall in a region of pure magnetic field. The tuning plunger was moved in small steps around the $Z = 0$ position and the value of '$K * B_{wall}$' in Eqn. (5) was determined. The plunger was then totally retracted and the frequency shift caused by the deep penetration was measured.

An effective penetration depth, $Z_{eff}$, may be defined by

$$Z_{eff} * \text{Area} * (K * B_{wall})^2 = f(Z=\infty) - f(Z=0) \qquad (7)$$

so that a penetration of depth $Z_{eff}$, if uniformly filled with wall strength magnetic field, would produce the same frequency shift as the infinitely deep penetration with the actual field.

For the 152 mm diameter penetration, $Z_{eff}$ was determined to be ≈ 29 mm, yielding the dimensionless value

$$\frac{Z_{eff}}{D} = 0.19 \pm 0.03$$

The rectangular penetration with the 2:1 cross section ratio yielded the values

$$\frac{Z_{eff}}{W} = 0.22 \pm 0.03 \text{ for } \frac{h}{W} = 0.5$$

$$= 0.16 \pm 0.04 \text{ for } \frac{h}{W} = 2.0$$

The errors quoted are estimates of systematic error and represent a 90% confidence level. Thus, if the wall fields and the field integrals are known for a cavity - for example, from a SUPERFISH calculation - then the frequency shift caused by deep wall penetrations with dimensions well below cutoff can be estimated.

## Field Probe Measurements

A selected set of $B_x$ and $B_z$ fields were measured, both along the axis and displaced from it. The $B_x$ fields were normalized in the following way: for $Z < 0$ (i.e., fields inside the $TM_{010}$ cavity) the measured field was divided by the field that would have existed without the penetration; for $Z > 0$ the measured field was divided by the unperturbed wall field. The $B_z$ fields were all normalized to the unperturbed wall field, $B_{wall}$.

The centre-axis longitudinal distributions of transverse magnetic field, $B_x(0,0,Z)$, are shown in Figs. 2 and 3 for a selection of penetration shapes and sizes. For field values less than half of the wall field ($Z/W > 0.2$) the decrease is exponential, with essentially the same exponent as the tuning plunger measurements. In Fig. 3, the effect of the aspect ratio on the central transverse field is shown. For the circular penetration, the distribution (see Fig. 4) is midway between the rectangular $Z/W = 0.5$ and 2.0 cases - i.e., approximately $Z/W = 1$, as expected.

The y (vertical) dependence of the transverse field, shown in Fig. 4, is relatively weak and in fact, at $(Z/D) \approx 0.1$ the transverse field for $x = 0$ is independent of y. This weak dependence is fortunate, because a drive loop or a field probe is usually oriented in the $x = 0$ plane, and the field integral which gives the voltage induced on the loop need not include y direction field variations. Thus the flux through a loop may be estimated by integrating the $y = 0$ curve in Fig. 4 over the function that defines the vertical loop dimensions.

$$\text{Flux} \approx D^2 * B_{wall} * \int \frac{B_x(0,0,U)}{B_{Norm}} Y_L(U)\, dU$$

unitless longitudinal dimensions

where $U = (Z/D)$ and $Y_L(U)$ is the unitless normalized loop size (i.e., the loop height divided by D) as a function of unitless longitudinal dimensions.

The series of longitudinal ($B_z$) and transverse ($B_x$) field measurements in Fig. 5 complete the basic characterization of magnetic fields in deep penetrations. The data were extrapolated to $(2x/D) = 1$ and $(2x/W) = 1$ to give an estimate of the wall field dependences (dotted lines on Figs. 4 and 5). These may be used to do an approximate calculation of the power losses on the walls of a penetration.

As an example, estimates were made of the ratio of the losses on the penetration walls relative to the loss that would have occurred on the piece of $TM_{010}$ cavity wall had it not been removed to put in the penetration. For a circular cross-section port, assuming a simple sine and cosine azimuthal dependence of the azimuthal and longitudinal wall fields, respectively, a loss ratio $0.57 \pm 0.06$ was calculated. For the rectangular cross section with $(h/W) = 0.5$, a similar calculation using the measured x coordinate dependences for the fields yields a value of $1.26 \pm 0.15$, meaning higher losses on the penetration than on the unperturbed cavity wall. The calculation for a thin vertical slot $[(h/W) >> 1]$ yields a value of $0.45 \pm 0.05$, suggesting a substantial reduction in the wall losses. The errors quoted are estimates of possible systematic error, both in the data and the numerical integration. Note that increased losses on the interior $TM_{010}$ cavity walls near the hole due to edge field enhancement are not included in these estimates.

## References

1. B.G. Chidley and G.E. McMichael, "RFQ1 Design Parameters", Proceedings of the 1984 Linear Accelerator Conference, GSI-84-11 (1984) 85.
2. R.M. Hutcheon, R.A. Vokes, T. Tran Ngoc and J.C. Brown, "The RF Design of a 270 MHz, CW Four Vane RFQ", these proceedings.
3. T. Moreno, "Microwave Transmission Design Data", Dover Publications Inc., New York (1958).
4. S. Ramo, J.R. Whinnery and T. Van Duzer, "Fields and Waves in Communication Electronics", published by John Wiley and Sons, Inc., New York (1965) 568.

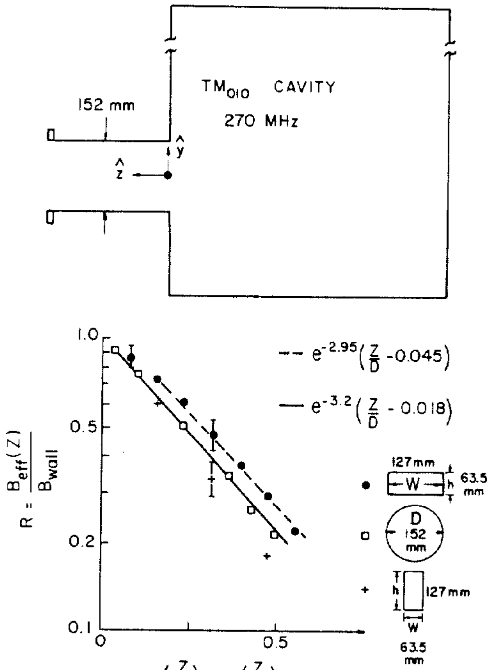


Fig. 1 The depth dependence of 'effective' magnetic field for three different shapes of penetrations, as derived from tuning plunger induced frequency shift measurements.

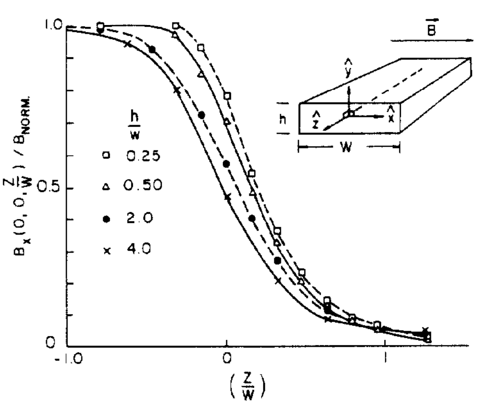


Fig. 3 The depth dependence of on-axis transverse magnetic field, $B_x$, for rectangular penetrations with varying aspect ratios.

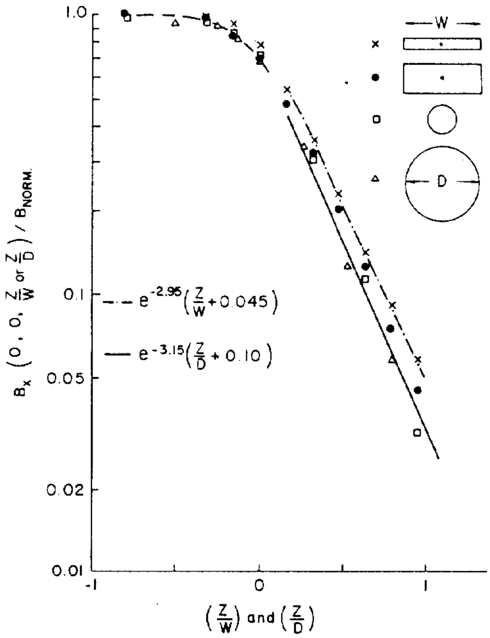


Fig. 2 The on-axis transverse magnetic field as a function of depth in four different penetrations, measured with a magnetic field probe. (See text for a definition of the normalizing field, $B_{Norm}$.)

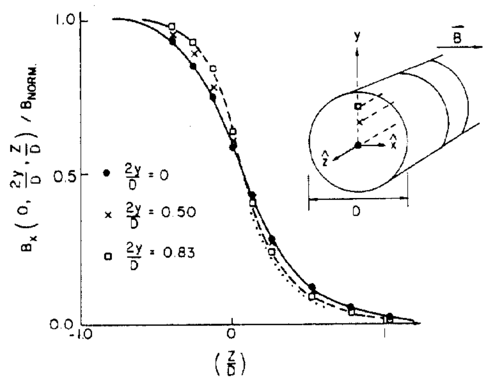


Fig. 4 The depth dependence of off-axis transverse magnetic field for a circular penetration. The dotted line is the wall field obtained by extrapolation.

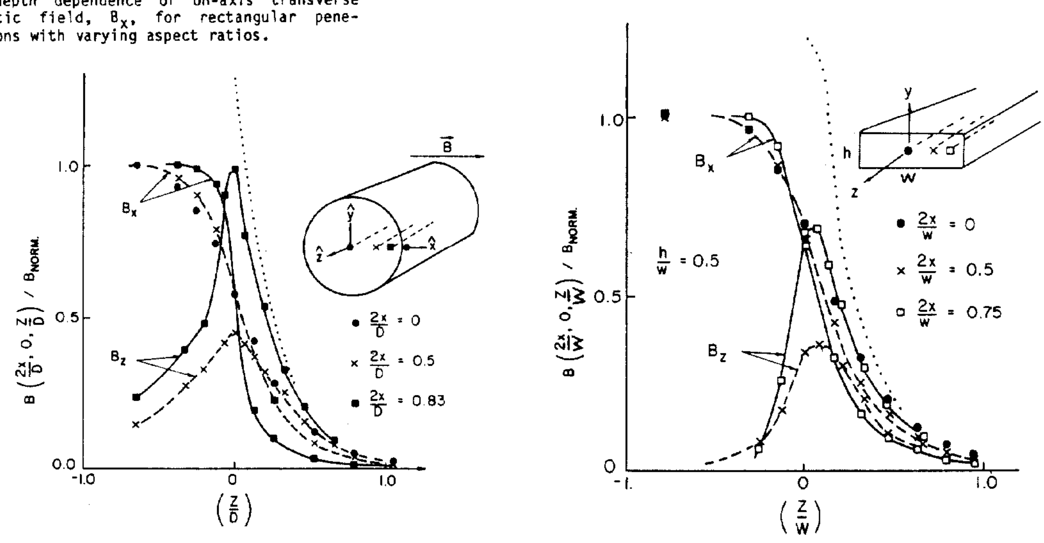


Fig. 5 The depth dependence of longitudinal, $B_z$, and transverse, $B_x$, off-axis magnetic fields in (a) a circular port and (b) a rectangular 2:1 aspect ratio port. The dotted lines are wall fields obtained by extrapolation.